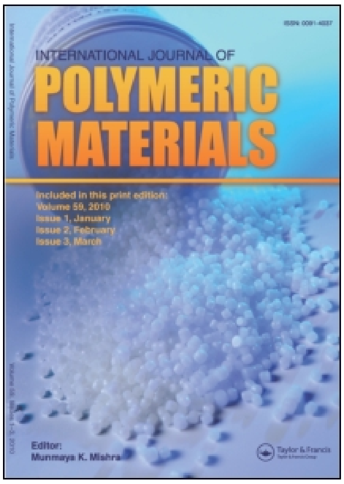

International Journal of Polymeric Materials
Publication details, including instructions for authors and subscription information:
http://www.informaworld.com/smpp/title~content=t713647664

Effect of Aging on the Mechanical Properties of UV Curable Optical Fiber Coatings

P. -A. Högström[a]; S. Karlsson[a]; U. W. Gedde[a]
[a] Department of Polymer Technology, Royal Institute of Technology, Stockholm, Sweden

To cite this Article Högström, P. -A. , Karlsson, S. and Gedde, U. W.(2000) 'Effect of Aging on the Mechanical Properties of UV Curable Optical Fiber Coatings', International Journal of Polymeric Materials, 46: 3, 403 — 421
To link to this Article: DOI: 10.1080/00914030008033884
URL: http://dx.doi.org/10.1080/00914030008033884

Intern. J. Polymeric Mater., 2000, Vol. 46, pp. 403–421
Reprints available directly from the publisher
Photocopying permitted by license only

Published by license under
the Gordon and Breach Science
Publishers imprint.
Printed in Malaysia.

Effect of Aging on the Mechanical Properties of UV Curable Optical Fiber Coatings

P.-A. HÖGSTRÖM, S. KARLSSON and U. W. GEDDE*

Department of Polymer Technology, Royal Institute of Technology, S-100 44 Stockholm, Sweden

(Received 18 November 1998)

A dual-layer urethane acrylate UV-cured coating is widely used to protect optical fibers because of its well-balanced mechanical properties, weathering resistance and rapid curing. The long-term mechanical behavior of fiber coatings is important for the reliability of optical fibers. Long-term exposure of UV-cured polyether urethane acrylate films was carried out in dry air and in water at elevated temperatures. Tensile testing was performed to reveal changes in mechanical properties and dynamic mechanical analysis to determine both the glass transition temperature and the crosslink density. The equilibrium swelling allowed assessment of the crosslink density. Tensile testing and strip force measurements were performed on virgin and aged optical fibers. Initially the fracture strengths of the secondary coatings increased under all aging conditions indicating post-curing reactions and the possible loss of uncrosslinked species. Aging under wet conditions led at a later stage to hydrolytic degradation of the network and to a decrease in the fracture stress. The equilibrium swelling and equilibrium modulus measurements showed good correlation with the changes in strength. The primary coatings showed a decrease in mechanical strength after only 2–4 weeks under all conditions.

Keywords: Acrylate; UV-curable coating; optical fiber; mechanical properties; degradation

INTRODUCTION

Polymer coatings are essential to protect optical glass fibers from mechanical stresses. Urethane acrylate resins are most commonly used

---

*Corresponding author.

because of their rapid curing. Usually they are deposited as a dual-layer coating on optical fibers used in telecommunications. The primary coating provides a soft buffer layer and protects the fiber against microbending while the secondary high modulus coating provides mechanical protection [1]. The effects of the structure of the coating on the mechanical properties of optical fibers have been reported [2–4]. The mechanical properties of the coatings are critical for the reliability of the fiber. Incompletely cured coatings or an unsuitable curing temperature may result in chemical changes in the network structure during service [5–8], *e.g.*, post-curing, migration of uncrosslinked species and thermo-oxidative and hydrolytic degradation [9–11]. This may lead to poor fiber performance; *e.g.*, transmission losses and handling problems due to reduced fiber strength, delamination and changes in coating strip force [12, 13].

This paper presents data for the mechanical properties of UV-cured urethane acrylate material subjected to oven aging and aging in water at elevated temperatures. The coatings were also characterized with respect to crosslink density and glass transition temperature using swelling measurements and dynamic mechanical analysis. The tensile strength and strippability of virgin and aged optical fibers were also measured.

EXPERIMENTAL

Four urethane acrylate-oligomer-based resins were used. The oligomers were polyether urethane diacrylates. Two of the resins were low-modulus primary coating materials (A and B) with long flexible polyether units. The remaining two were high-modulus secondary coating materials (C and D) with shorter polyether linking units.

Each coating was drawn down on a Mylar film supported by a glass plate using an Erichsen film applicator. A thick glass plate acts as a heat sink and promotes vitrification of the coating materials if the glass transition temperature of the coating exceeds the cure temperature [14, 15]. The substrate film was used to prevent vitrification of the secondary coatings and to allow punching of the coating films for tensile testing specimens. The coatings were cured in a box with a fused silica window to 100% of their ultimate modulus using a F300

UV-source (D-bulb, 120 W/cm) from Fusion Systems. The box was purged with nitrogen for five minutes before curing in order to reduce the concentration of dissolved oxygen in the acrylate resin. The coating thickness was measured with a Mitutoyo micro-thickness meter. UV-cured coating samples were aged for different periods of time ranging from 1 week to 32 weeks. The aging treatments were carried out in moderately circulating dry air at 95 and 115°C and in deionized water at 85 and 95°C. Fiber aging studies were conducted on 250 µm dual-coated optical fibers, with coating systems A/C and B/D respectively, for the same time periods in deionized water at 95°C. The temperature was controlled to an accuracy of ± 2°C.

The tensile testing was performed on an Instron 5566 tensile testing machine equipped with a 2663 non-contacting video extensometer and pneumatic grips. The measurements were performed at a cross-head speed of 1 mm/min for the high-modulus secondary coatings and at 10 mm/min for the low-modulus primary coatings using a grip separation of 25.4 mm. The test specimens, ASTM D638V, with a thickness of approximately 0.1 mm, were conditioned prior to testing for 24 h at 50 ± 5% RH and 23 ± 1°C. The two parameter Weibull distribution function, $1-F(\sigma) = \exp[-(\sigma/\sigma_{0.63})^b]$, was fitted to the fracture stress and fracture strain data consisting of at least 6 data points for each sample and the fracture stress and fracture strain corresponding to the cumulative frequency $F = 0.63$ (scale parameter, $\sigma_{0.63}$ and $\varepsilon_{0.63}$ respectively) and the shape parameter (b) were determined by the maximum-likelihood method.

The dynamic mechanical analysis was performed on the high-modulus secondary coatings on a Polymer Laboratories MK II instrument. The measurements were made in the single cantilever mode with a grip distance of 10 mm. The 20 × 10 mm rectangular strips with a thickness of 0.1 mm were preconditioned at 60°C for one hour. A temperature scan was run from − 20°C to 130°C at a rate of 2°C/min. The storage modulus and loss tangent were obtained at a frequency of 1 Hz and a dynamic strain of 16 µm peak to peak. The mean values for three samples were calculated.

20 × 20 mm samples, 0.1 mm thick, were extracted in methylethyl ketone (MEK) for 16 hours to remove uncrosslinked species, dried, weighed and then submerged in MEK for 16 hours. Solvent was then removed from the surface and the sample mass was recorded at

5 second intervals. An evaporation curve, *i.e.*, mass as a function of time, was then fitted using a third degree polynomial to estimate the sample mass directly after removal from the solvent.

The tensile strength and strippability of the optical fibers were measured according to IEC standard 793-1-3, Optical fibres. The tensile strength was determined on an Instron 4302 tensile testing machine at a strain rate of 10%/min with a gauge length of 500 mm. The strip force was obtained at a stripping rate of 500 mm/min and the length of fiber stripped was 50 mm. The fibers were preconditioned for a minimum of 24 h at 50% RH and 23°C.

RESULTS AND DISCUSSION

High-modulus Secondary Coatings

The high-modulus secondary coating constitutes the outer part, provides environmental protection and distributes localized mechanical stresses. Chemical and physical changes in the coating may endanger the reliability of the optical fiber.

Aging in air resulted in a significant increase in fracture stress and a simultaneous decrease in fracture strain (Figs. 1a and 1b). Coating C showed at 115°C a pronounced increase in fracture stress and a decrease in fracture strain during the first 500 to 1000 h, after which these quantities remained essentially constant (Fig. 1a). There was a small but significant decrease in the fracture stress (as well as an increase in fracture strain) after ~5500 h of aging at 115°C. Aging of coating C at 95°C resulted in slower changes in these parameters but in the same direction as was observed for aging at 115°C. The "equilibrium" levels in fracture stress and strain were reached after 2000 – 3000 h at 95°C (Fig. 1a). The initial change in fracture stress and strain was strictly proportional to the square root of the aging time at both 95 and 115°C. The slope coefficients showed a temperature dependence, which could be expressed in terms of activation energies of 43 kJ/mol (fracture stress) and 22 kJ/mol (fracture strain). Coating D showed basically a similar development of fracture stress and strain with aging time, the only difference being that the initial changes in both fracture stress and fracture strain showed a weaker temperature

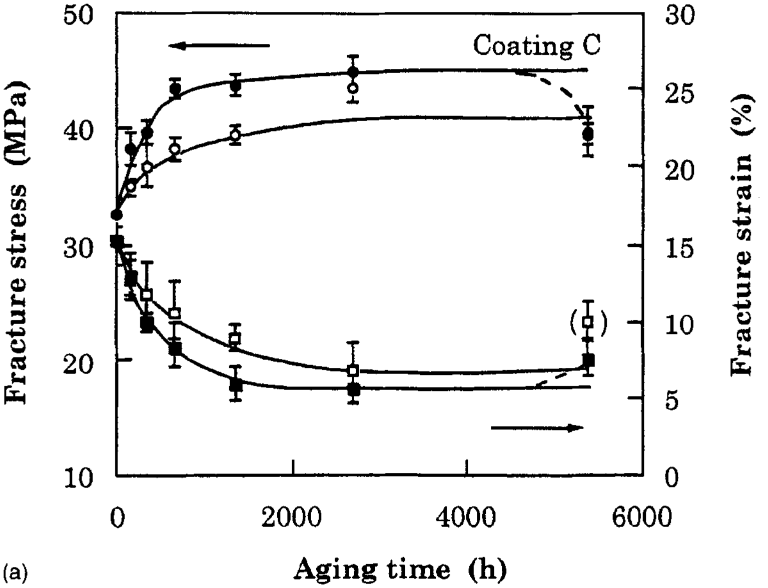

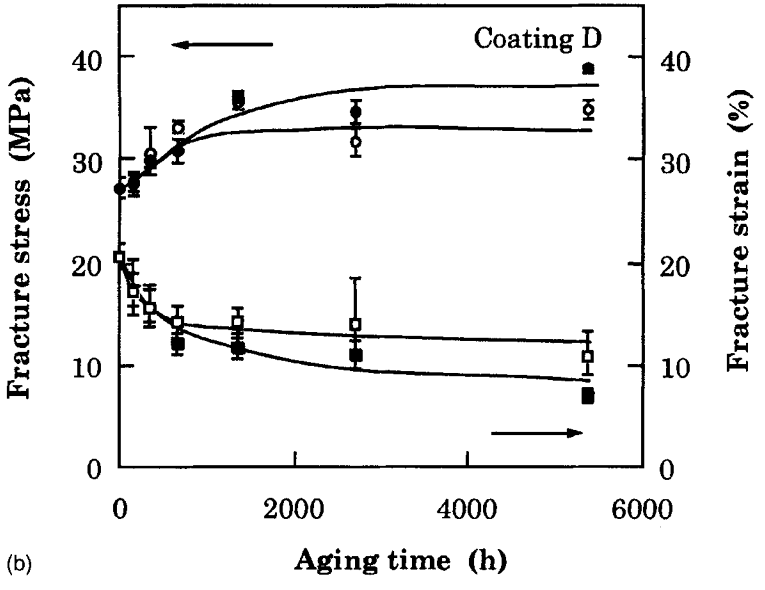

FIGURE 1 Fracture stress and strain for a) coating C, and b) coating D, aged in dry air at 95°C (unfilled symbols) and at 115°C (filled symbols) as a function of aging time. The error bars indicate the 95% confidence intervals.

dependence (Fig. 1b). The equilibrium levels of fracture stress and fracture strain showed some temperature dependence; the equilibrium stress increased and the equilibrium strain decreased with increasing aging temperature (Figs. 1a and 1b).

The equilibrium (rubber) modulus (E_0) is, according to rubber elasticity theory, strictly proportional to the number of chain segments (chains surrounded by crosslink junction points) per unit volume, *i.e.*, to number of crosslinks per unit volume [16]. The equilibrium degree of swelling decreases according to the Flory-Rehner equation in a slightly non-linear fashion with increasing number of crosslinks per unit volume [16]. The variation in solute concentration in the swollen samples in this study was however small, and the equilibrium degree of swelling decreased in an approximately linear manner with increasing number of crosslinks per unit volume within this limited concentration range. Figures 2a and 2b show that the effective number of crosslinks per unit volume increased in a non-linear (retarding) fashion with

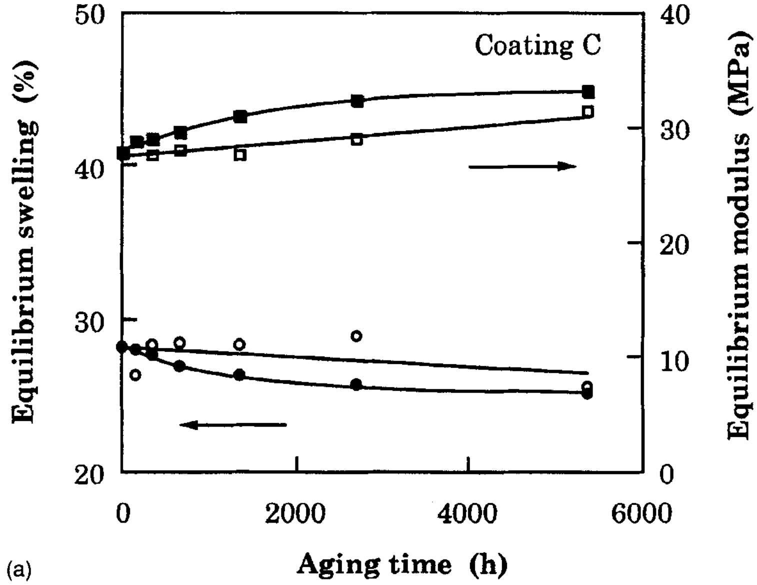

(a)

FIGURE 2 Equilibrium swelling and modulus for a) coating C, and b) coating D, aged in dry air at 95°C (unfilled symbols) and at 115°C (filled symbols) as a function of aging time.

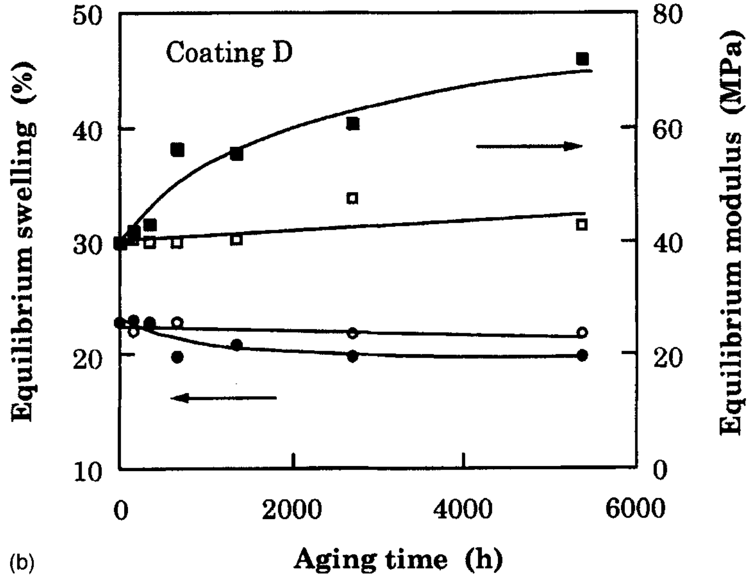

FIGURE 2 (Continued).

increasing aging time at 115°C for both coatings C and D. The changes in the network structure during aging at 95°C were substantially smaller but in the same direction as was observed after aging at 115°C. It may be assumed that some unreacted species had reacted during aging and that the concentration of unreacted species before aging (c_0) should be proportional to $E_0(\text{final}) - E_0(t = 0)$. The concentration ($c$) of unreacted species at time t is proportional to $E_0(\text{final}) - E_0(t)$. Similar relationships were established using the equilibrium swelling data. Different kinetics expressions, diffusion-controlled $[c/c_0 \propto t^{1/2}]$, zero order $[c/c_0 \propto t]$, first order $[c/c_0 = \exp(-kt)]$ and second order $[c_0/c \propto t]$, were tested, and clearly the first three failed whereas the expression for the second order kinetics could be fitted to the experimental rubber modulus and swelling data (Fig. 3). Note that the fitting was only possible for the data for the samples aged at 115°C, except for coating D for which the swelling data showed too great a scatter to permit meaningful fitting. Samples aged at 95°C showed too little change in E_0 to allow critical testing of the different kinetics expressions. The data thus seems to support the

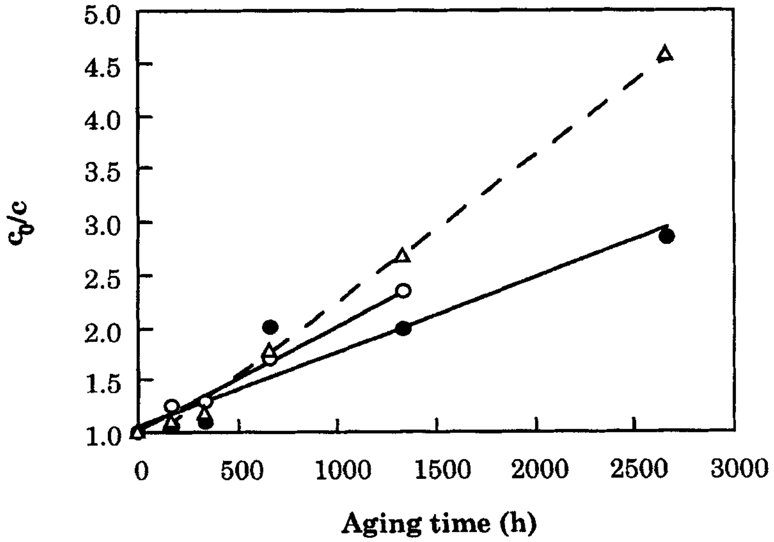

FIGURE 3 The ratio of the concentrations of unreacted groups before aging (c_0) and after aging (c) as a function of aging time. The concentrations were calculated from equilibrium modulus data (○ material C, 115°C; ● material D, 115°C) and from equilibrium swelling data (Δ material C, 115°C).

conclusion that aging in air induces post-curing reactions and the formation of a denser network.

The increase in the network density of the stiff coating materials was also evident in an increase in the glass transition temperature. The increase in fracture stress and fracture strain with aging time displayed in Figures 1a and 1b is also consistent with the observed and almost simultaneous increase in network density (Figs. 2a and 2b). After the longest aging exposure (5300 h ≈ 32 weeks), coating C showed a decrease in fracture stress and an increase in fracture strain, indicating possible oxidative network degradation. It was noticed however, that these changes in the solid state mechanical properties were not accompanied by any signs of network degradation as revealed by the rubber modulus or swelling data.

Specimens exposed to aging in water showed initially an increase in fracture stress and a decrease in fracture strain (Figs. 4a and 4b). The mechanical behavior of the specimens aged in water is similar to the behavior of those aged in air during the first 1000 h, despite the

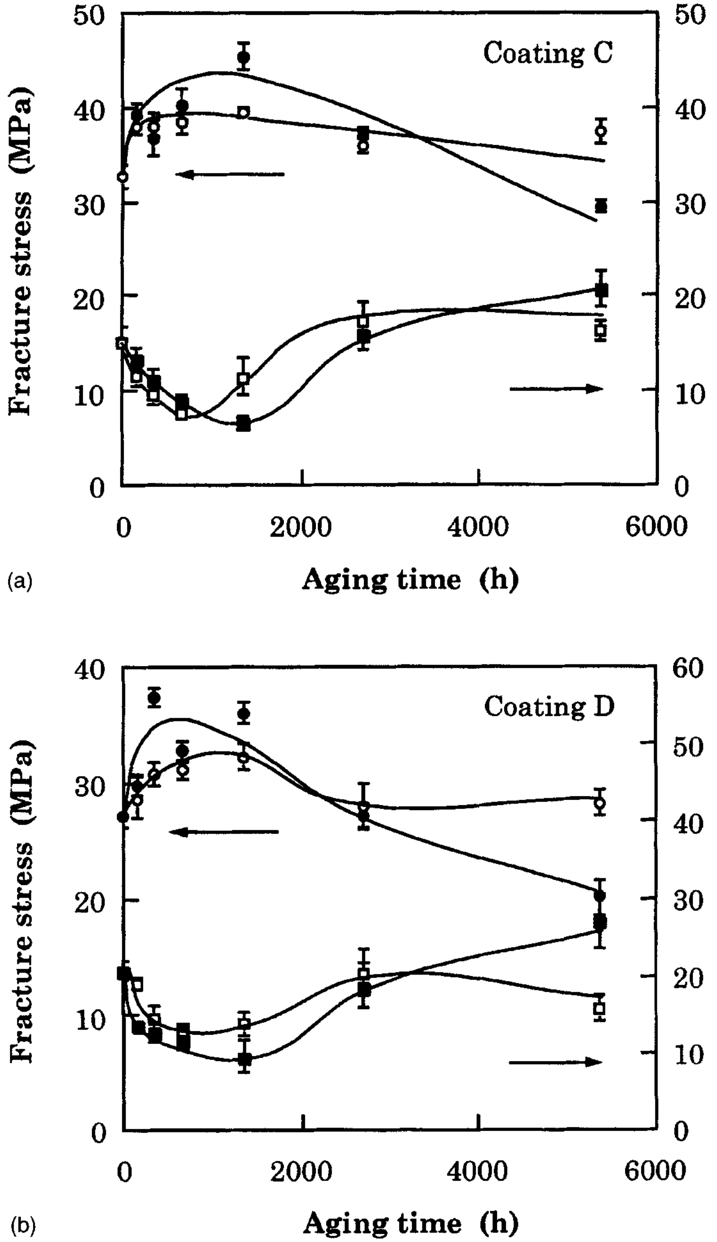

FIGURE 4 Fracture stress and strain for a) coating C, and b) coating D, aged in water at 85°C (unfilled symbols) and at 95°C (filled symbols) as a function of aging time.

temperature difference, – air aging was performed at 95 and 115°C and water aging at 85 and 95°C (Figs. 1 and 4). Specimens exposed to more extensive aging (> 1000 h) showed a significant reduction in fracture stress and an increase in fracture strain with increasing aging time (Figs. 4a and 4b). The drop in fracture stress is more pronounced for the specimens aged at the higher temperature (95°C). The time for the onset of the deterioration of the mechanical properties showed almost no temperature dependence (Figs. 4a and 4b). Figure 5 shows that the reason for the deterioration of the mechanical properties is network degradation, which is particularly pronounced for coating D, which showed a drop in elastic modulus from the initial value of 38 MPa to only 15 MPa after 5300 h of exposure in water at 95°C. These data indicate that a substantial portion of the chains were broken leaving less than 50% of the network junctions effective. The glass transition temperature increased during wet aging but this was not as

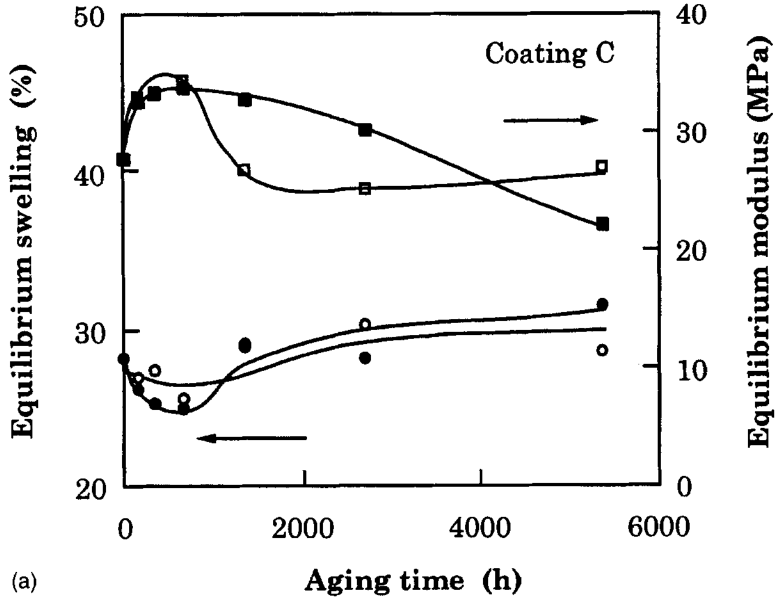

FIGURE 5 Equilibrium swelling and modulus for a) coating C, and b) coating D, aged in water at 85°C (unfilled symbols) and at 95°C (filled symbols) as a function of aging time.

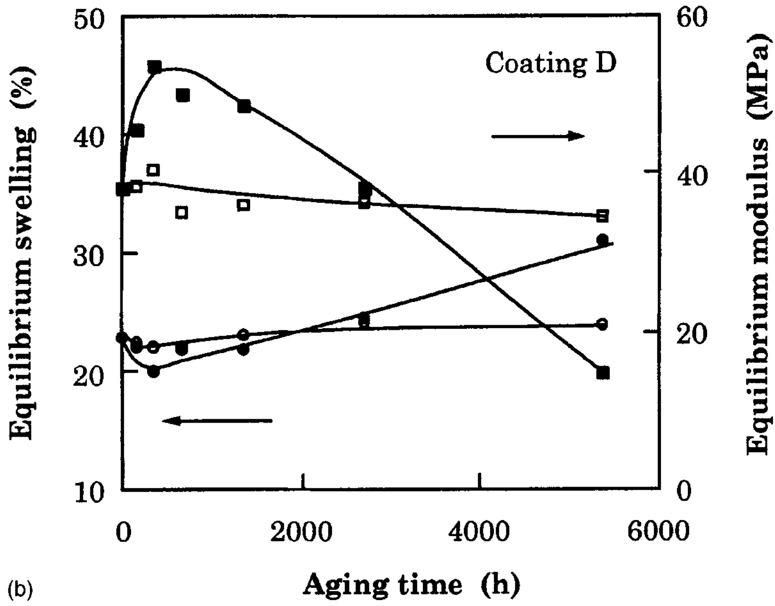

FIGURE 5 (Continued).

pronounced as for the coatings aged under dry conditions. This is probably due to the counteracting action of hydrolytic chain scission.

To conclude this it can be stated that aging in air of high-modulus coating materials resulted in post-curing and a denser network with a higher fracture stress and a lower fracture strain, whereas aging under wet conditions initially triggered the post-curing reactions but later led to extensive hydrolytic network degradation causing pronounced deterioration of the mechanical properties.

Low-modulus Primary Coatings

Degradation of the inner so-called primary coating may lead to greater attenuation losses due to microbending and also to handling problems associated with stripping from the optical fiber. The different primary coating materials (coatings A and B) showed essentially the same aging characteristics under the different aging conditions tested. Figures 6a and 6b show the deterioration of the mechanical properties under dry aging conditions. The initial increase in fracture stress (and

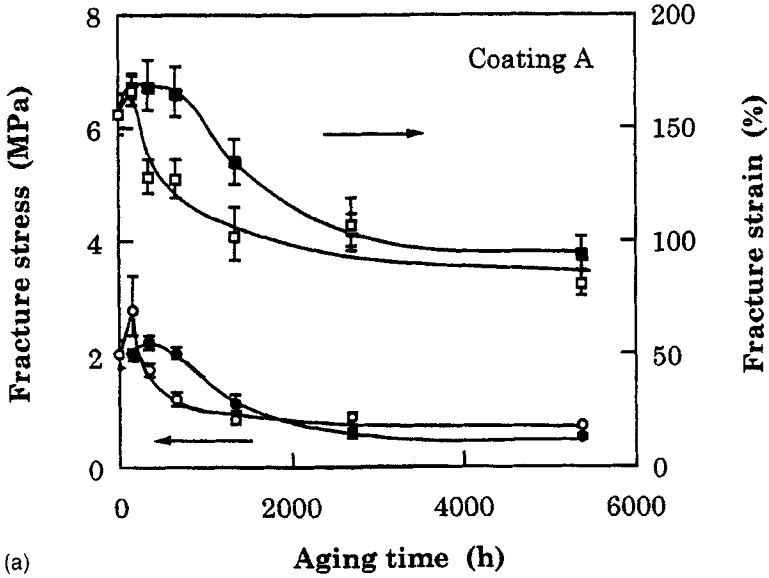

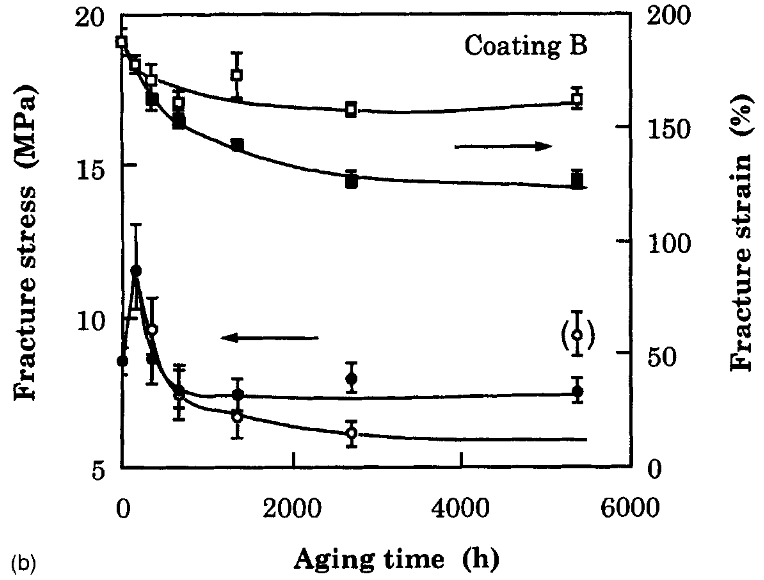

FIGURE 6 Fracture stress and strain for a) coating A, and b) coating B, aged in dry air at 95°C (unfilled symbols) and at 115°C (filled symbols) as a function of aging time.

decrease in fracture strain) shown by the high-modulus coating materials is almost completely absent in this case. Whereas the high-modulus materials vitrify during curing leaving unreacted species in the glassy structure, the low-modulus materials stay above their glass transition temperature during the curing and a smaller fraction of the functional groups are expected to remain unreacted after curing. The low-modulus materials showed a decrease in both fracture stress and strain with increasing aging time (Figs. 6a and 6b), indicating a network degradation. The aging in water was particularly severe to the materials, causing an extensive loss of mechanical properties and loss of material integrity after only 8 to 16 weeks (1300 to 2600 h) (Figs. 7a and 7b).

Figures 8 and 9 present rubber modulus and equilibrium swelling data for coating A, aged in dry air and in water, respectively. Note that this material is in the rubbery state and that Young's modulus is equal to the equilibrium (elastic) modulus. Coating A showed extensive network degradation on aging at 115°C; the modulus dropped by 50% and the degree of swelling increased from 200% to 250% over aging period covered (5300 h). Aging at 95°C caused only a very small

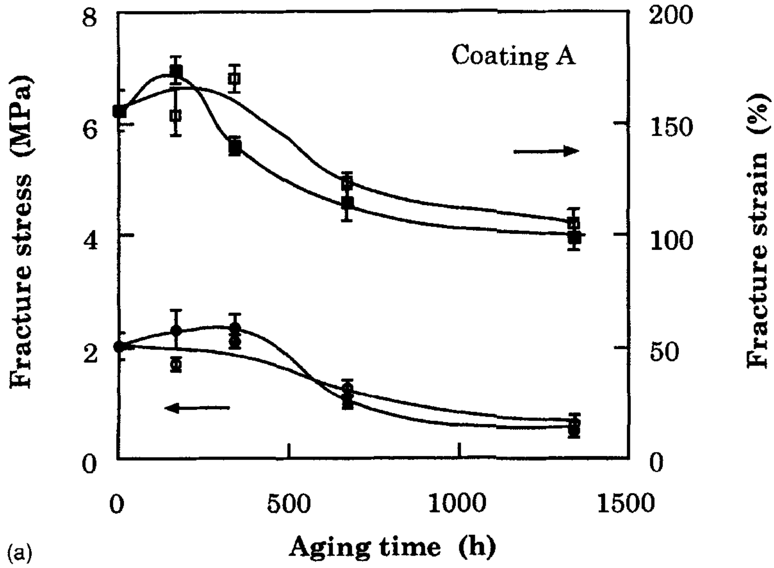

FIGURE 7 Fracture stress and strain for a) coating A, and b) coating B, aged in water at 85°C (unfilled symbols) and at 95°C (filled symbols) as a function of aging time.

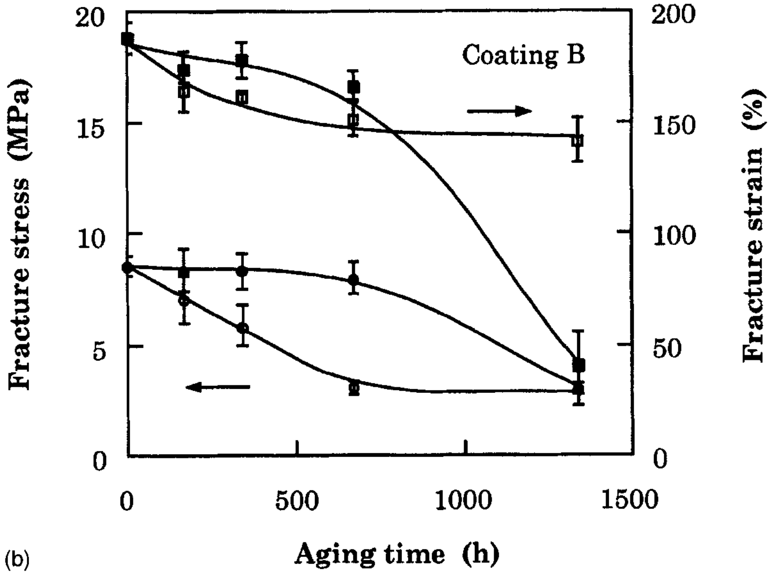

FIGURE 7 (Continued).

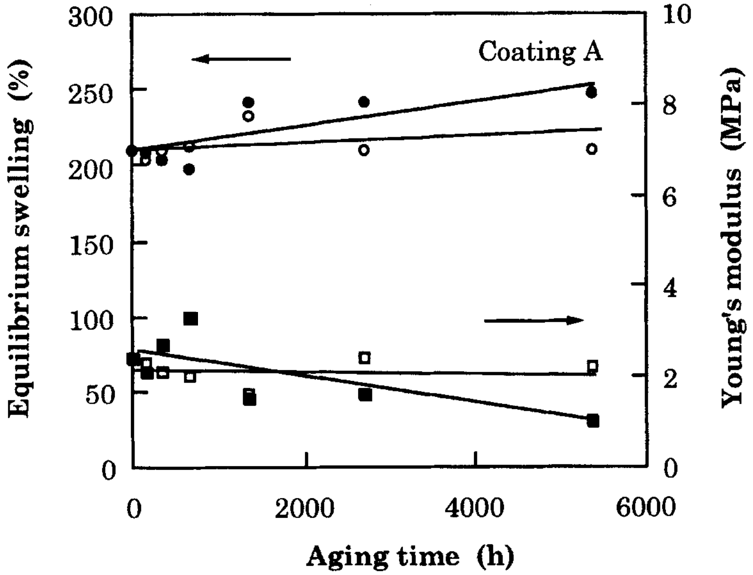

FIGURE 8 Equilibrium swelling and modulus for coating A, aged in dry air at 95°C (unfilled symbols) and at 115°C (filled symbols) as a function of aging time.

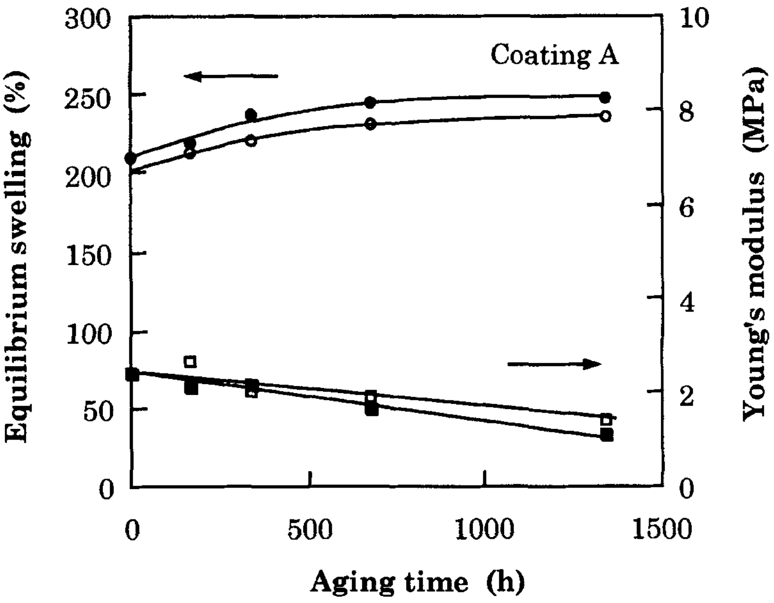

FIGURE 9 Equilibrium swelling and modulus for coating A, aged in water at 85°C (unfilled symbols) and at 95°C (filled symbols) as a function of aging time.

decrease in modulus and a slight increase in the degree of swelling, which may seem surprising in view of the extensive deterioration in the mechanical properties occurring on aging at 95°C (Fig. 6a).

Coating B was in the glass transition region and no elastic modulus data were obtained for this material. However, it was noticed that coating B originally exhibited a significantly higher Young's modulus than material A, and also that the Young's modulus data for coating B increased with increasing aging time under all aging conditions tested. Equilibrium swelling data for coating B are shown in Figures 10 and 11. Aging under dry conditions caused a decrease in degree of swelling, possibly due to oxidative crosslinking.

Fiber Studies

The tensile strength of the fiber coated with materials A and C showed initially a very small increase followed by a small decrease (~10%). Further water aging beyond 2000 h caused no further decrease in

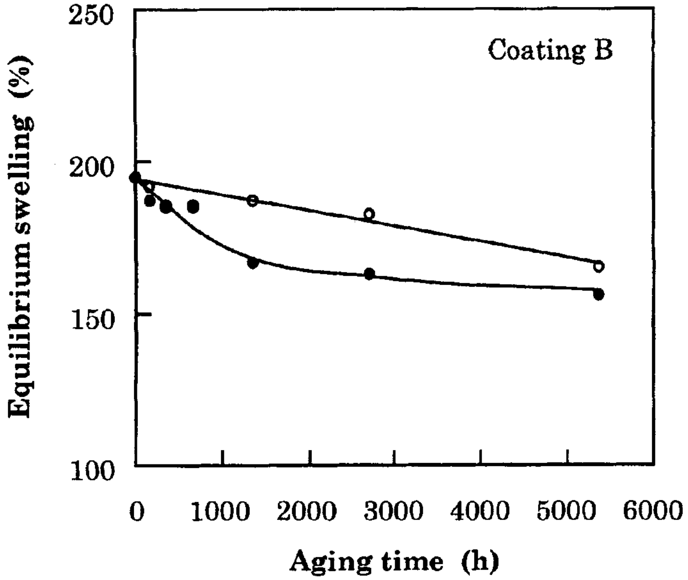

FIGURE 10 Equilibrium swelling for coating B, aged in dry air at 95°C (unfilled symbols) and at 115°C (filled symbols) as a function of aging time.

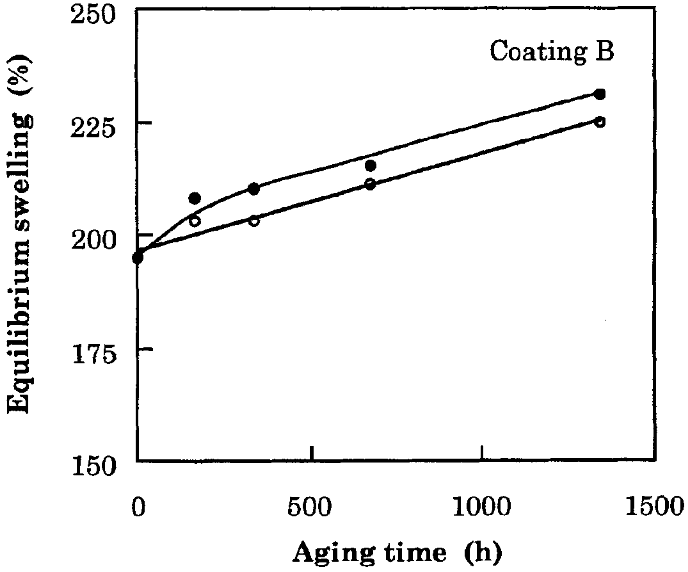

FIGURE 11 Equilibrium swelling for coating B, aged in water at 85°C (unfilled symbols) and at 95°C (filled symbols) as a function of aging time.

tensile strength (Fig. 12). Coatings A and C both showed an extensive deterioration in their mechanical properties during similar aging. It thus seems that the mechanical properties, although inferior to those of the virgin materials, were sufficient to protect the glass from water-induced degradation of the Si—O-linkages. The fiber coated with materials B and D showed a rapid and extensive loss in tensile strength after water aging (Fig. 12). The rates of degradation of these materials in water were essentially no different from those of the A and C coatings (see previous sections). It is suggested that the high modulus of the B coating led to early delamination and the presence of free water at the glass interface. Other factors, *e.g.*, differences in coating pH may also be influential. This permits scission of Si—O bonds at the interface causing a reduction in the tensile strength [17, 18].

The strip force data in Figure 13 showed a correlation with the modulus of the primary coating materials. The fiber coated with

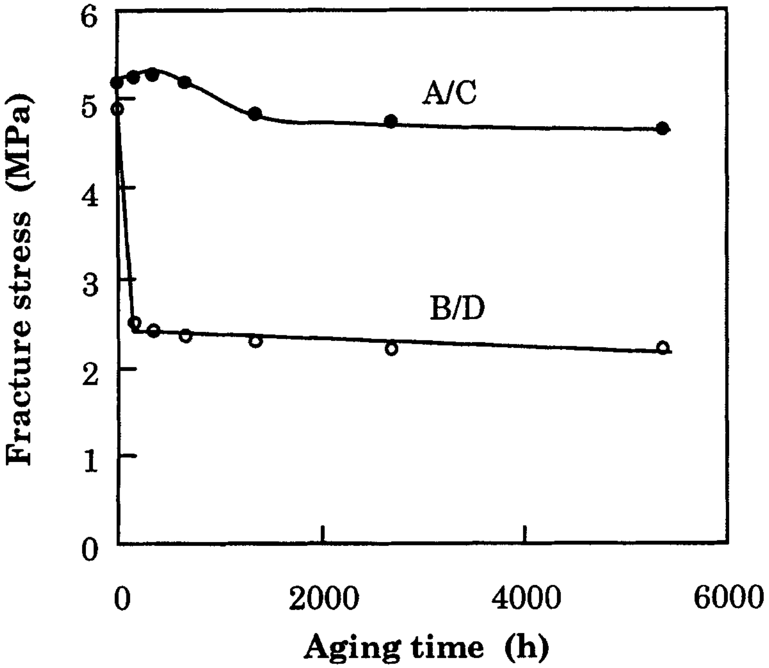

FIGURE 12 Fracture stress for fibers aged in water at 95°C as a function of aging time. Coating systems A/C (filled symbols) and B/D (unfilled symbols).

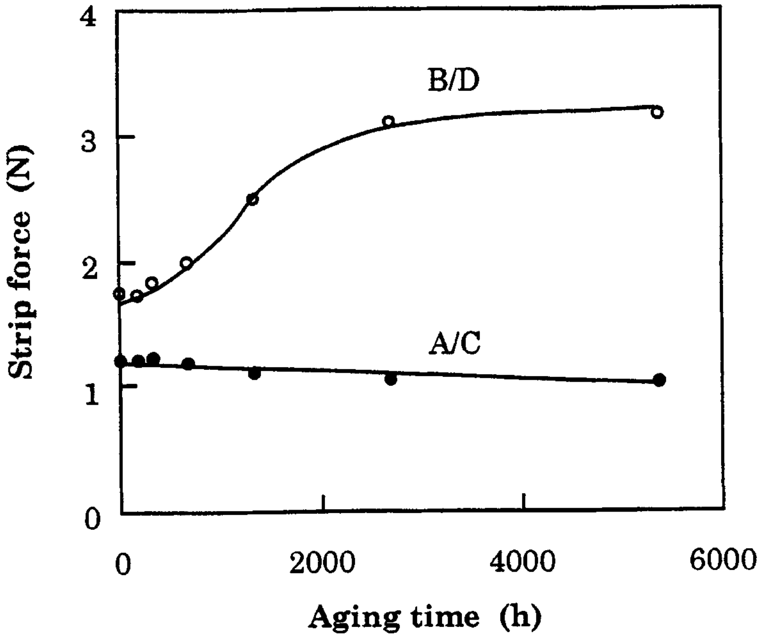

FIGURE 13 Strip force of fibers aged in water at 95°C as a function of aging time. Coating systems A/C (filled symbols) and B/D (unfilled symbols).

material B showed an increase in strip force with increasing aging time, which correlated well with the increase in modulus observed for the B material. The fiber coated with material A showed a lowering in strip force on wet aging due to the softening of the A material.

CONCLUSIONS

The effects of aging on the mechanical properties of poly (ether urethane acrylate) coatings were studied in films and *in situ* on coated optical glass fibers. Aging in air of the high modulus secondary coatings at elevated temperatures caused post-curing. This led to a stiffer material with lower fracture strain. Aging in water for longer times resulted in progressive network degradation by hydrolysis. The primary coatings showed decreasing tensile strength after 2–4 weeks under all test conditions. The strip force of the fibers showed patterns of changes on aging similar to those of the primary coating film modulus. An increase in film modulus was accompanied by an increase in the strip force.

Acknowledgements

This study has been sponsored by the Swedish Board for Technical and Industrial Development (NUTEK, grant P71-5), Ericsson Cables AB, Hudiksvall and Telia Net AB, Stockholm (Sweden). Karin Nygård-Skalman, Ericsson Cables AB and Jan Björkman, Telia Net AB are acknowledged for valuable discussions.

References

[1] Blyler, L. L. Jr. and Aloisio, C. J. (1987). *Chemtech.*, **17**, 680.
[2] Yuce, H. H. and Hasse, A. D. (1988). *37th Intern. Wire Cable Symp Proc.*, p. 732.
[3] Yuce, H. H., Plitz, I. M., Frantz, R. A. and Andrejco, M. (1990). *39th Intern. Wire Cable Symp. Proc.*, p. 715.
[4] Cocchini, F. (1994). *Polym. Eng. Sci.*, **34**, 414.
[5] Overton, B. J., Taylor, C. R. and Muller, A. J. (1989). *Polym. Eng. Sci.*, **29**, 1165.
[6] Frantz, R. A., Plitz, I. M., Yuce, H. H. and Gebizlioglu, O. S. (1992). *41st Intern. Wire Cable Symp. Proc.*, p. 279.
[7] Komiya, Z., Takasugi, Y., Ukachi, T. and Paternack, G. (1993). *42nd Intern. Wire Cable Symp. Proc.*, p. 531.
[8] Takase, H., Hashiguchi, Y., Takasugi, Y., Saito, N. and Ukachi, T. (1994). *43rd Intern. Wire Cable Symp. Proc.*, p. 72.
[9] Högström, P.-A., Karlsson, S. and Gedde, U. W. (1996). *45th Intern. Wire Cable Symp. Proc.*, p. 464.
[10] Simoff, D. A., Chan, M. G., Chapin, J. T. and Overton, B. J. (1989). *Polym. Eng. Sci.*, **29**, 1177.
[11] Szum, D. S., Chawla, C. P., Bishop, T. E., Murray, K. P. and Zimmerman, J. M. (1990). *39th Intern. Wire Cable Symp. Proc.*, p. 703.
[12] Hsiao, J. M., Wang, S. I., Chen, K. Y. Chang, T. C., Fann, D. M. and Lin, Y. C. (1992). *41st Intern. Wire Cable Symp. Proc.*, p. 435.
[13] Murata, A., Oohashi, K. and Araki, S. (1996). *45th Intern. Wire Cable Symp. Proc.*, p. 322.
[14] Enns, J. B. and Gillham, J. K. (1983). *J. Appl. Polym. Sci.*, **28**, 2567.
[15] Szum, D. M. (1994). *43rd Int. Wire Cable Symp. Proc.*, p. 59.
[16] Gedde, U. W. (1995). Polymer Physics, London, Chapman & Hall.
[17] Yuce, H. H. (1992). *41st Intern. Wire Cable Symp. Proc.*, p. 605.
[18] Griffioen, W. (1992). *41st Intern. Wire Cable Symp. Proc.*, p. 622.